

Effective application of machine learning to bacterial 16S rRNA gene sequencing data

Running title: Machine learning methods in microbiome studies

Begüm D. Topçuoğlu¹, Nicholas A. Lesniak¹, Mack Ruffin³, Jenna Wiens², Patrick D. Schloss^{1†}

† To whom correspondence should be addressed: pschloss@umich.edu

1. Department of Microbiology and Immunology, University of Michigan, Ann Arbor, MI 48109

2. Department of Electrical Engineering and Computer Science, University of Michigan, Ann Arbor, MI 48109

3. Department of Family Medicine and Community Medicine, Penn State Hershey Medical Center,

Hershey, PA

Abstract

Machine learning (ML) modeling of the human microbiome has the potential to identify microbial biomarkers and aid in diagnosis of many diseases such as inflammatory bowel disease, diabetes, and colorectal cancer. Progress has been made towards developing ML models that predict health outcomes using bacterial abundances, but inconsistent adoption of training and evaluation methods call the validity of these models into question. Furthermore, there appears to be a preference by many researchers to favor increased model complexity over interpretability. To overcome these challenges, we trained seven models that used fecal 16S rRNA sequence data to predict the presence of colonic screen relevant neoplasias (SRNs; n=490 patients, 261 controls and 229 cases). We developed a generalizable pipeline to train, validate and interpret the models. To show the effect of model selection, we assessed the predictive performance, interpretability, and training time of L2-regularized logistic regression, L1 and L2-regularized support vector machines (SVM) with linear and radial basis function kernels, decision trees, random forest, and extreme gradient boosted trees (XGBoost). The random forest model performed best at detecting SRNs with an AUROC of 0.695 [IQR 0.651-0.739] but was slow to train (83.2 h) and difficult to interpret. Despite its simplicity, L2-regularized logistic regression followed random forest in predictive performance with an AUROC of 0.680 [IQR 0.625-0.735], trained faster (12 min), and was more interpretable. Our analysis showed that ML models should be chosen based on the goal of the study, as the choice will inform expectations of performance and interpretability.

20 **Importance**

21 Prediction of health outcomes using machine learning (ML) is rapidly being adopted in human
22 microbiome studies. However, these ML models are likely overoptimistic in terms of quantifying
23 predictive performance. Moreover, there is a trend towards using black box models such as random
24 forest and neural networks without a discussion of the difficulty of interpreting such models when
25 trying to identify microbial biomarkers of disease. This work represents a step towards developing
26 better ML practices in microbiome research by implementing a rigorous pipeline and emphasizing
27 the importance of selecting ML models that reflect the goal of the study. These concepts are not
28 particular to the study of health outcomes but can also be applied to environmental microbiology
29 studies.

Background

As the number of people represented in human microbiome datasets grow, there is an increasing desire to use microbiome data to diagnose diseases. However, the structure of the human microbiome is remarkably variable AMONG individuals to the point where it is often difficult to identify the bacterial populations that are associated with diseases using traditional statistical models. This variation is likely due to the ability of many bacterial populations to fill the same niche such that different populations cause the same disease in different individuals. Furthermore, a growing number of studies have shown that it is rare for a single bacterial species to be associated with a disease. Instead, subsets of the microbiome account for differences in health. Traditional statistical approaches do not adequately account for the variation in the human microbiome and typically consider the protective or risk effects of each bacterial population individually. Recently, machine learning models (ML) have grown in popularity among microbiome researchers because of the large amount of data that can now be generated and because the models are effective at accounting for the interpersonal microbiome variation and the ecology of the disease.

ML models can be used to increase our understanding of the variation in the structure of existing data and in making predictions about new data. Researchers have used ML models to diagnose and understand the ecological basis of diseases such as liver cirrhosis, colorectal cancer, inflammatory bowel diseases, obesity, and type 2 diabetes (1–16, 16–18). The task of diagnosing an individual relies on a rigorously validated model. However, there are common methodological and reporting problems that arise when applying ML to such data, that need to be addressed for the field to progress. These problems include a lack of transparency in which methods are used and how these methods are implemented; evaluating models without a separate held-out test data; large variation between the predictive performance on different folds of cross-validation; and large variation between cross-validation and testing performances. Nevertheless, the microbiome field is making progress to avoid some of these pitfalls including validating their models on independent datasets (7, 18, 19) and introducing ways to better use ML tools (20–23). More work is needed to further improve reproducibility and minimize overestimating for model performance.

Among microbiome researchers, the lack of justification when selecting a modelling approach has

been due to an implicit assumption that more complex models are better. This has resulted in a trend towards using models such as random forest and deep neural networks (2, 11, 24–26) over simpler models such as logistic regression or other linear models (18, 22, 27). Although complex models may in some cases, capture important non-linear relationships and therefore yield better predictions, they may result in black boxes that lack interpretability. Such models require post hoc explanations to quantify the importance of each feature in making predictions. Depending on the goal of the modeling, researchers may choose to use different approaches. For example, researchers trying to identify the populations of microbiota associated with disease may desire a more interpretable model, whereas clinicians may emphasize predictive performance. Nonetheless, it is important to understand the tradeoff and accepting that this tradeoff may be minimal (28, 29). It is important for researchers to justify their choice of modelling approach.

To showcase a rigorous ML pipeline and to shed light on how ML model selection can affect modeling results, we performed an empirical analysis comparing seven modeling approaches with the same dataset and pipeline. We built three linear models with different forms of regularization: L2-regularized logistic regression and L1 and L2-regularized support vector machines (SVM) with a linear kernel. We also trained four non-linear models: SVM with radial basis function kernel, a decision tree, random forest and XGBoost. We compared their predictive performance, interpretability, and training time. To demonstrate the performance of these modeling approaches and our pipeline, we used data from a previously published study that sought to classify individuals as having normal colons or colonic lesions based on the 16S rRNA gene sequences collected from fecal samples (3). This dataset was selected because it is a relatively large collection of individuals (N=490) connected to a clinically significant disease where there is ample evidence that the disease is driven by variation in the microbiome (1, 3, 4, 30). With this dataset we developed a ML pipeline that can be used in many different scenarios for training and evaluating models. This framework can be easily applied to other host-associated and environmental microbiome datasets.

Results

Model selection and pipeline construction We established a reusable ML pipeline for model selection and evaluation, focusing on seven different commonly used supervised learning algorithms [Figure 1].

First, we randomly split the data into training and test sets so that the training set consisted of 80% of the full dataset, while the test set was composed of the remaining 20% [Figure 1]. To maintain the distribution of controls and cases found in the full dataset, we performed stratified splits. For example, our full dataset included 490 individuals. Of these, 261 had normal colons (53%) and 229 had a screen relevant neoplasia (SRN; 46.7%). A training set included 393 individuals, of which 209 had an SRN (53%), while the test set was composed of 97 individuals of which 52 had an SRN (54%). The training data was used to build and select the models and the test set was used for evaluating the model.

We trained seven different models using the training data [Table 1]. We focused on different classification algorithms and regularization methods. Regularization helps to prevent overfitting by penalizing a model that fits the training data too well. For regularized logistic regression and SVM with a linear kernel, we used L2-regularization to keep all potentially important features. For comparison, we also trained an L1-regularized SVM with a linear kernel. L1-regularization on microbiome data led to a sparser solution (i.e., forced many coefficients to zero). To explore the potential for non-linear relationships among features to improve classification, we trained tree-based models including a decision tree, a random forest, and XGBoost and an SVM with a non-linear kernel.

Model selection required tuning hyperparameters. Hyperparameters are parameters which need to be specified or tuned by the user, in order to train a model for a specific modeling problem. For example, when using regularization, (C) is a hyperparameter that indicates the penalty for overfitting. Hyperparameters are tuned using the training data to find the best model. We selected hyperparameters by performing repeated five-fold cross-validation (CV) on the training set [Figure 1]. The five-fold CV was also stratified to maintain the overall case and control distribution. We

chose the hyperparameter values that led to the best average CV predictive performance using the area under the receiver operating characteristic curve (AUROC) [Figure S1 and S2]. The AUROC ranges from 1.0, where the model perfectly distinguishes between cases and controls, to 0, where the model's predictions are perfectly incorrect. An AUROC value of 0.5 indicates that model's predictions are no different than random. To select hyperparameters, we performed a full grid search for hyperparameter settings when training our models. Default hyperparameter settings in previously developed ML packages in R, Python, and MATLAB programming languages may be inadequate for effective application of classification algorithms and need to be optimized for each new ML task. In the example of L1-regularized SVM with linear kernel [Figure S1], the model showed large variability between different regularization strengths (C).

Once hyperparameters were selected, we trained the model using the full training dataset and applied the final model to the held-out data to evaluate the testing predictive performance of each model. The data-split, hyperparameter selection, training and testing steps were repeated 100 times to obtain a reliable and robust interpretation of model performance [Figure 1].

Predictive performance and generalizability of the seven models. We evaluated the predictive performance of the seven models to classify individuals as having normal colons or SRNs [Figure 2]. The random forest model had significantly higher test AUROC values than the other models for detecting SRNs (Wilcoxon rank sum test, $p < 0.01$). The median AUROC of the random forest model was 0.695 (IQR 0.044). L2-regularized logistic regression, XGBoost, L2-regularized SVM with linear and radial basis function kernel AUROC values were not significantly different from one another and had median AUROC values of 0.680 (IQR 0.055), 0.679 (IQR 0.052), 0.678 (IQR 0.056) and 0.668 (IQR 0.056), respectively. L1-regularized SVM with linear kernel and decision tree had significantly lower AUROC values than the other ML models with median AUROC of 0.650 (IQR 0.066) and 0.601 (IQR 0.059), respectively [Figure 2]. Interestingly, these results demonstrate that the most complex model (XGBoost) did not have the best performance and that the most interpretable models (L2-regularized logistic regression and SVM with linear kernel) performed nearly as well non-linear models.

To evaluate the generalizability of each model, we compared the median cross-validation AUROC

to the median testing AUROC. If the difference between the cross-validation and testing AUROCs was large, then that could indicate that the models were overfit to the training data. The difference in median AUROCs was 0.021 in L1-regularized SVM with linear kernel, followed by SVM with radial basis function kernel and decision tree with a difference of 0.007 and 0.006, respectively [Figure 2]. These differences are relatively small and gives us confidence in our estimate of the generalization performance of the models.

To evaluate the variation in the estimated performance, we calculated the range of AUROC values for each model using 100 data-splits. The range among the testing AUROC values within each model varied by 0.230 on average across the seven models. If we had only done a single split, then there is a risk that we could have gotten lucky or unlucky in estimating model performance. For instance, the lowest AUROC value of the random forest model was 0.593 whereas the highest was 0.810. These results showed that depending on the data-split, the testing performance can vary [Figure 2]. Therefore, it is important to employ multiple data splits when estimating generalization performance.

To show the effect of sample size on model generalizability, we compared cross-validation AUROC values of L2-regularized logistic regression and random forest models when we subsetting our original study design with 490 subjects to 15, 30, 60, 120, and 245 subjects [Figure S3]. The variation in cross-validation performance within both models at lower sample sizes was larger than when the full collection of samples was used to train and validate the models. Because of the high dimensionality of the microbiome data (6920 OTUs), large sample sizes can lead to better models.

Interpretation of each ML model. Interpretability is related to the degree to which humans can understand the reasons behind a model prediction (31–33). Because we often use ML models not just to predict a health outcome but also to identify the biomarkers for a disease, model interpretation becomes crucial for microbiome studies. ML models decrease in interpretability as they increase in complexity. In this study we used two methods to help interpret our models.

First, we interpreted the feature importance of the linear models (L1 and L2-regularized SVM with linear kernel and L2-regularized logistic regression) using the median rank of absolute feature weights for each OTU [Figure 3]. We also reviewed the signs of feature weights to determine

whether an OTU was associated with classifying a subject as being healthy or having an SRN. It was encouraging that many of the highest ranked OTUs were shared across these three models, (e.g. OTU 50, 426, 609, 822, 1239). The benefit of this approach was that the results of the analysis were based on the trained model parameters and provided information regarding the sign and magnitude of the impact of each OTU. However, this approach is only possible with linear models.

Second, to analyze non-linear models we interpreted the feature importance using permutation importance. Whereas the absolute feature weights were determined from the trained models, here we measured importance using the held-out test data. Permutation importance analysis is a posthoc explanation of the model, in which we randomly permuted groups of perfectly correlated features together and other features individually across the two groups in the held-out test data. We then calculated how much the predictive performance of the model (i.e, testing AUROC values) decreased when each OTU or group of OTUs was randomly permuted. We ranked the OTUs based on how much the median testing AUROC decreased when it was permuted; the OTU with the largest decrease ranked highest [Figure 4]. Among the twenty OTUs with the largest impact, there was only one OTU (OTU 822) that was shared among all of the models; however, we found three OTUs (OTU 58, 110, 367) that were important in each of the tree-based models. Similarly, the random forest and XGBoost models, shared four of the most important OTUs (OTU 2, 12, 361, 477). Permutation analysis results also revealed that with the exception of the decision tree model, removal of any individual OTU had minimal impact on model performance. For example, if OTU 367 was permuted across the samples in the decision tree model, the median AUROC dropped from 0.601 to 0.525. In contrast, if the same OTU was permuted in the random forest model, the AUROC only dropped from 0.695 to 0.680. In this case, similar to previous studies (22, 34), it was not possible to distinguish between health and disease using a single OTU. Although permutation analysis allowed us to gauge the importance of an OTU, the analysis was post-hoc (i.e. done using the test data) and these results did not allow us to directly interrogate the models to know whether an OTU was associated with classifying a subject as being healthy or having an SRN.

To further highlight the differences between the two interpretation methods, we used permutation importance to interpret the linear models [Figure S4]. When we analyzed the L1-regularized SVM with linear kernel model using feature rankings based on weights [Figure 3] and permutation

importance [Figure S4], 17 of the 20 top OTUs (e.g. OTU 609, 822, 1239) were deemed important by both interpretation methods. Similarly, for the L2-regularized SVM and L2-regularized logistic regression, 9 and 12 OTUs, respectively, were shared among the two interpretation methods. Although permutation analysis does not allow us to determine the weight or the sign of the features, these results indicate that both methods are consistent in selecting the most important OTUs.

The computational efficiency of each ML model. We compared the training times of the seven ML models. As expected, the training times increased with the complexity of the model and the number of potential hyperparameter combinations. Also, the linear models trained faster than non-linear models [Figures S1-S2; Figure 5].

Discussion

There is a growing awareness that many human diseases and environmental processes are not driven by a single organism but are the product of multiple bacterial populations. Traditional statistical approaches are useful for identifying those cases where a single organism is associated with a process. In contrast, ML methods offer the ability to incorporate the structure of the microbial communities as a whole and identify associations between community structure and disease state. If it is possible to classify communities reliably, then ML methods also offer the ability to identify those microbial populations within the communities that are responsible for the classification. However, the application of ML in microbiome studies is still in its infancy and the field needs to develop a better understanding of different ML methods, their strengths and weaknesses, and how to implement them.

To address these needs, we developed an open-sourced framework to ML models. using this pipeline, we benchmarked seven ML models and showed that the tradeoff between model complexity and performance may be less severe than originally hypothesized. In terms of predictive performance, the random forest model had the best AUROC compared to the other six models. However, the second-best model was L2-regularized logistic regression with a median AUROC

221 difference of only 0.015 compared to random forest. While our implementation of random forest
222 took 83.2 hours to train, our L2-regularized logistic regression trained in 12 minutes. In terms of
223 interpretability, random forest is a non-linear ML model and is most often explained using post-hoc
224 methods such as permutation importance. On the other hand, using L2-regularized logistic
225 regression we ranked the importance of each OTU based on their feature weights. Comparing
226 many different models showed us that the most complex model was not necessarily the best model
227 for our ML task.

228 As we set out to select the best model, we established a pipeline that can be generalized to any
229 modeling method that predicts a binary health outcome. We performed a random data-split to
230 create a training set (80% of the data) and a held-out test set (20% of the data), which we used to
231 evaluate predictive performance. We repeated this data-split 100 times to measure the possible
232 variation in predictive performance. During the training, we tuned the model hyperparameters with
233 a repeated five-fold cross-validation. Despite the high number of features microbiome datasets
234 typically have, the models we built with this pipeline were generalizable as shown by the good test
235 AUROCs.

236 We highlighted the importance of model interpretation to gain greater biological insights into
237 microbiota-associated diseases. In this study we showcased two different interpretation methods:
238 ranking each OTU by (i) their absolute weights in the trained models and (ii) their impact on
239 the predictive performance based on permutation importance. Human-associated microbial
240 communities have complex correlation structures which create collinearity in the datasets. This
241 can hinder our ability to reliably interpret models because the feature weights of correlated OTUs
242 are influenced by one another (35). To capture all important features, once we identify highly
243 ranked OTUs, we should review their relationships with other OTUs. These relationships will
244 help us generate new hypotheses about the ecology of the disease and test them with follow-up
245 experiments. When we used permutation importance, we took collinearity into consideration by
246 grouping correlated OTUs to determine their impact as a group. We grouped OTUs that had a
247 perfect correlation with each other however, we can reduce the correlation threshold to further
248 investigate the relationships among correlated features. It is important to know the correlation
249 structures of the data to avoid misinterpreting the models. This is likely to be a particular problem

with shotgun metagenomic datasets where collinearity will be more pronounced due to many genes being correlated with one another because they come from the same chromosome. To identify the true underlying microbial factors of a disease, it is crucial to do correlation analyses and further experimentation for biological validation.

In this study, we did not consider all possible modeling approaches. However, the principles highlighted throughout this study apply to other ML modeling tasks with microbiome data. For example, we did not evaluate multicategory classification methods to predict non-binary outcomes. We could have trained models to differentiate between people with normal colons and those with adenomas or carcinomas ($k=3$ categories). We did not perform this analysis because the clinically relevant diagnosis grouping was between patients with normal colons and those with SRNs. Furthermore, as number of classes increases, more samples are required for each category to train an accurate model. We also did not use regression-based analyses to predict a non-categorical outcome. We have previously used such an approach to train random forest models to predict fecal short-chain fatty acid concentrations based on microbiome data (36). Our analysis was also limited to shallow learning methods and did not explore deep learning methods such as neural networks. Deep learning methods hold promise (11, 37, 38) but microbiome datasets often suffer from having many features and small sample sizes, which can result in overfitting.

Our framework provides a reproducible structure to investigators wanting to train, evaluate, and interpret their own ML models to generate hypotheses regarding which OTUs might be biologically relevant. However, deploying microbiome-based models to make clinical diagnoses or predictions is a significantly harder and distinct undertaking. For example, we currently lack standardized methods to collect patient samples, generate sequence data, and report clinical data. We are also challenged by the practical constraints of OTU-based approaches. The de novo algorithms commonly in use are slow, require considerable memory, and result in different OTU assignments as new data are added. Finally, we also need independent validation cohorts to test the performance of a diagnostic model. To realize the potential for using ML approaches with microbiome data, it is necessary that we direct our efforts to overcome these challenges.

Our study highlights the need to make educated choices at every step of developing a ML model

with microbiome data. We created an aspirational rubric that researchers can use to identify potential pitfalls when using ML in microbiome studies and ways to avoid them [Table S1]. We have highlighted the trade-offs between model complexity and interpretability, the need for tuning hyperparameters, the utility of held-out test sets for evaluating predictive performance, and the importance of considering correlation structures in datasets for reliable interpretation. Furthermore, we underscored the importance of proper experimental design and methods to help us achieve the level of validity and accountability we want from models built for patient health.

Materials and Methods

Data collection and study population. The original stool samples described in our analysis were obtained from patients recruited by Great Lakes-New England Early Detection Research Network (Reference from Mack?). Stool samples were provided by adults who were undergoing a scheduled screening or surveillance colonoscopy. Participants were recruited from: Toronto (ON, Canada), Boston (MA, USA), Houston (TX, USA), and Ann Arbor (MI, USA). Patients' colonic health was visually assessed by colonoscopy with bowel preparation and tissue histopathology of all resected lesions. We assigned patients into two classes: those with normal colons and those with screen relevant neoplasias (SRNs). The normal class included patients with normal colons or non-advanced adenomas whereas the SRN class included patients with advanced adenomas or carcinomas (reference for SRN?). Patients with an adenoma greater than 1 cm, more than three adenomas of any size, or an adenoma with villous histology were classified as having advanced adenomas. There were 172 patients with normal colonoscopies, 198 with adenomas, and 120 with carcinomas. Of the 198 adenomas, 109 were identified as advanced adenomas. Together 261 patients were classified as normal and 229 patients were classified as having a SRN.

16S rRNA gene sequencing data. Stool samples provided by the patients were used for 16S rRNA gene sequencing to measure bacterial population abundances. The sequence data used in our analyses were originally generated by Baxter et al. (available through NCBI Sequence Read Archive [SRP062005], 2015). The OTU abundance table was generated by Sze et al (34), who processed the 16S rRNA sequences in mothur (v1.39.3) using the default quality filtering methods, identifying

and removing chimeric sequences using VSEARCH, and assigning to OTUs at 97% similarity using the OptiClust algorithm (39–41); (https://github.com/SchlossLab/Sze_CRCMetaAnalysis_mBio_2018/blob/master/data/process/baxter/baxter.0.03.subsample.shared). These OTU abundances were the features we used to predict colorectal health of the patients. There were 6920 OTUs. OTU abundances were subsampled to the size of the smallest sample and normalized across samples such that the highest abundance of each OTU would be 1 and lowest would be 0.

Model training and evaluation. Models were trained using the caret package (v.6.0.81) in R (v.3.5.0). We modified the caret code to calculate decision values instead of predicted probabilities for models generated using L2-regularized SVM with linear kernel and L1-regularized SVM with linear kernel. These changes were necessary to calculate AUROC values for SVMs. The code for these changes on L2-regularized SVM with linear kernel and L1-regularized SVM with linear kernel models are available at https://github.com/SchlossLab/Topcuoglu_ML_XXX_2019/blob/master/data/caret_models/svmLinear3.R and at https://github.com/SchlossLab/Topcuoglu_ML_XXX_2019/blob/master/data/caret_models/svmLinear4.R, respectively.

For hyperparameter selection, we started with a granular grid search. Then we narrowed and fine-tuned the range of each hyperparameter. A full grid search was needed to avoid large variation in prediction performance. For L2-regularized logistic regression, L1 and L2-regularized SVM with linear and radial basis function kernels, we tuned the **cost** hyperparameter which determines the regularization strength where smaller values specify stronger regularization. For SVM with radial basis function kernel we also tuned **sigma** hyperparameter which determines the reach of a single training instance where for a high value of sigma, the SVM decision boundary will be dependent on the points that are closest to the decision boundary. For the decision tree model, we tuned the **depth of the tree** where deeper the tree, the more splits it has. For random forest, we tuned the **number of features** to consider when looking for the best tree split. For XGBoost, we tuned for **learning rate** and the **fraction of samples** to be used for fitting the individual base learners. Recently developed tools such as Hyperband help researchers with hyperparameter selection that can be incorporated to microbiome studies (42) .

The computational burden during model training due to model complexity was reduced by

parallelizing segments of the ML pipeline. We parallelized the training of each data-split. This allowed the 100 data-splits to be processed through the ML pipeline simultaneously at the same time for each model. It is possible to further parallelize the cross-validation step for each hyperparameter setting if limited by computational resources.

Permutation importance workflow. We calculated a Spearman's rank-order correlation matrix and defined correlated OTUs as having perfect correlation (correlation coefficient = 1 and $p < 0.01$). Non-correlated OTUs were permuted individually whereas correlated ones were grouped together and permuted at the same time.

Statistical analysis workflow. Data summaries, statistical analysis, and data visualizations were performed using R (v.3.5.0) with the tidyverse package (v.1.2.1). We compared the AUROC values of the seven ML models by Wilcoxon rank sum tests to determine the best predictive performance.

Code availability. The code for all sequence curation and analysis steps including an Rmarkdown version of this manuscript is available at https://github.com/SchlossLab/Topcuoglu_ML_XXX_2019/.

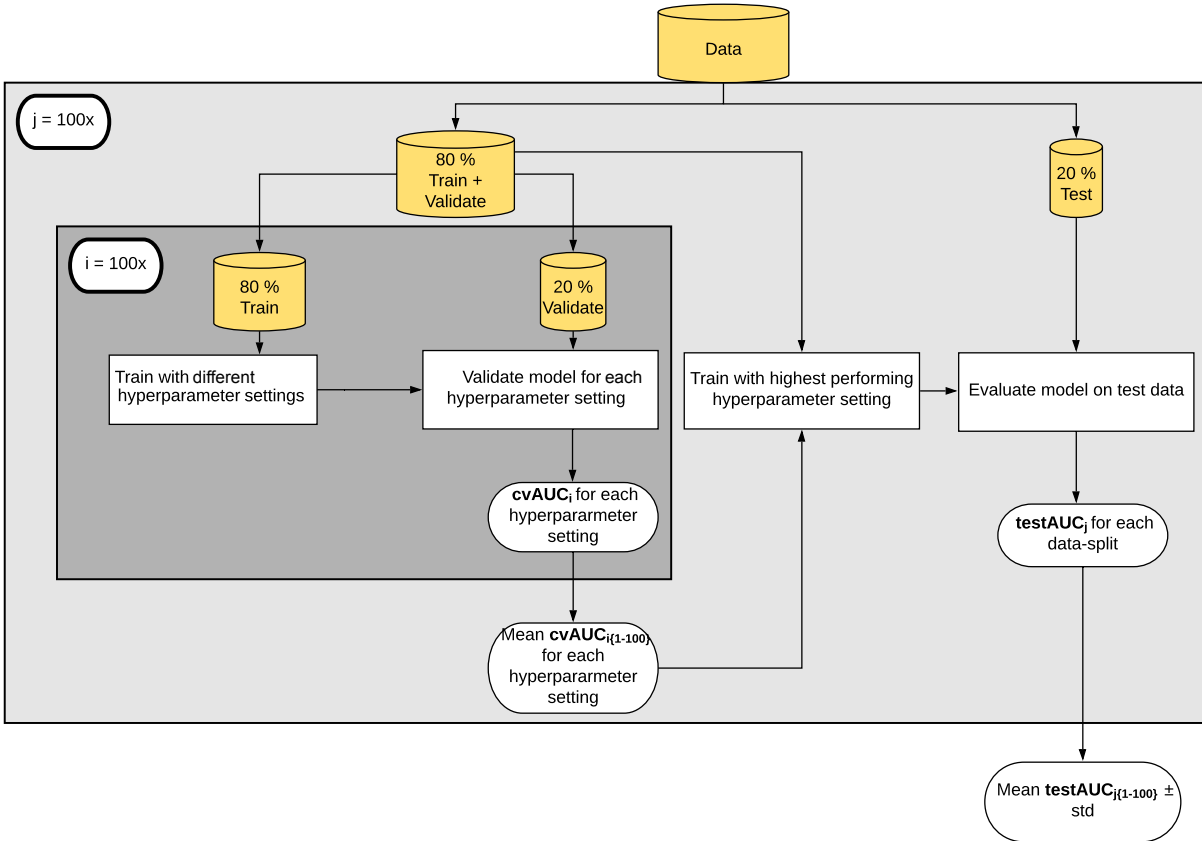


Figure 1. Machine learning pipeline. We split the data to create a training (80%) and held-out test set (20%). The splits were stratified to maintain the overall label distribution. We performed five-fold cross-validation on the training data to select the best hyperparameter setting and then used these hyperparameters to train the models. The model was evaluated on the held-out data set. Abbreviations: cvAUC, cross-validation area under the receiver operating characteristic curve.

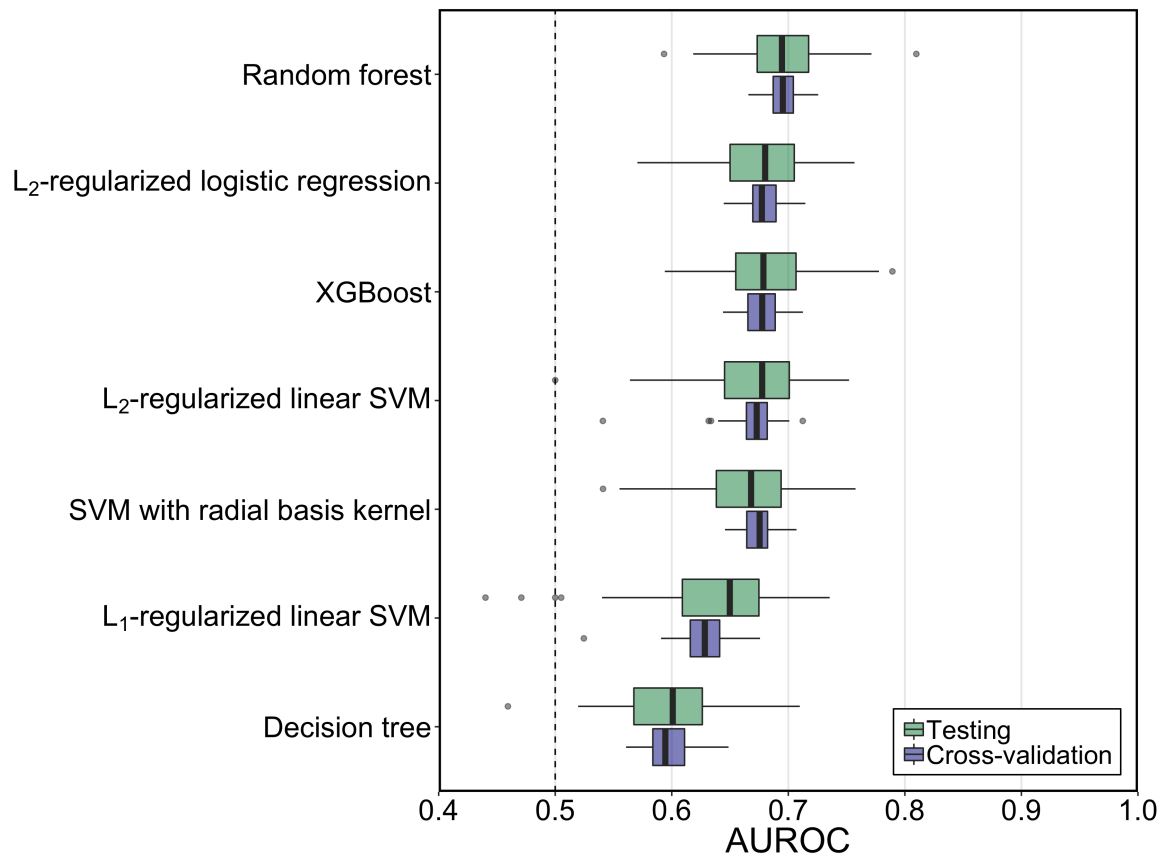


Figure 2. Generalization and classification performance of ML models using AUROC values of all cross validation and testing performances. The median AUROC for diagnosing individuals with SRN using bacterial abundances was higher than chance (depicted by horizontal line at 0.50) for all the ML models. Predictive performance of random forest model was higher than other ML models. The boxplot shows quartiles at the box ends and the median as the horizontal line in the box. The whiskers show the farthest points that were not outliers. Outliers were defined as those data points that are not within 1.5 times the interquartile ranges.

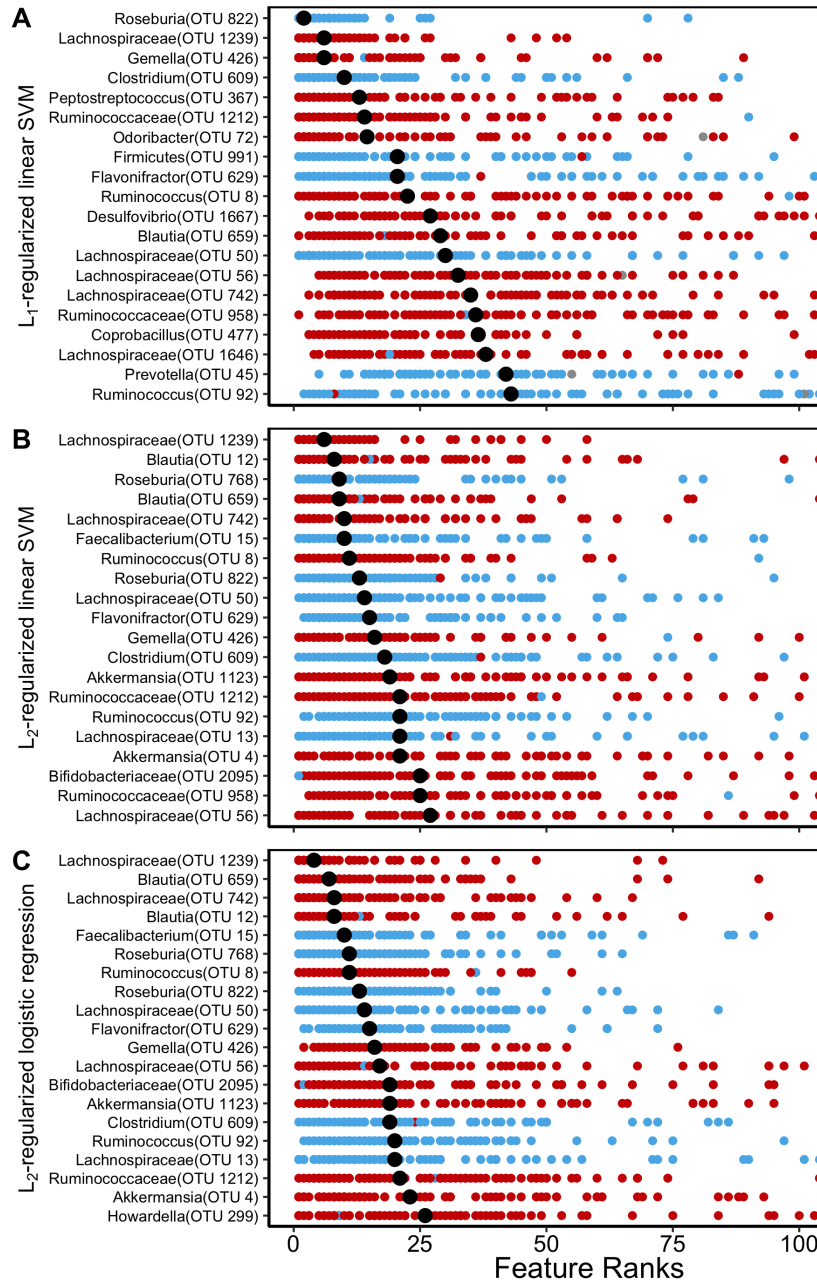


Figure 3. Interpretation of the linear ML models. The absolute feature weights of (A) L₂-regularized logistic regression, (B) L₁-regularized SVM with linear kernel, and (C) L₂-regularized SVM with linear kernel were ranked from highest rank, 1, to lowest rank, 100, for each data-split. The feature ranks of the 20 highest ranked OTUs based on their median ranks (median shown in black) are reported here. OTUs that are associated with classifying a subject as being healthy had negative signs and were shown in blue. OTUs that are associated with classifying a subject having an SRN had positive signs and were shown in red. Some of the same OTUs were identified as

368 important in all of the linear models.

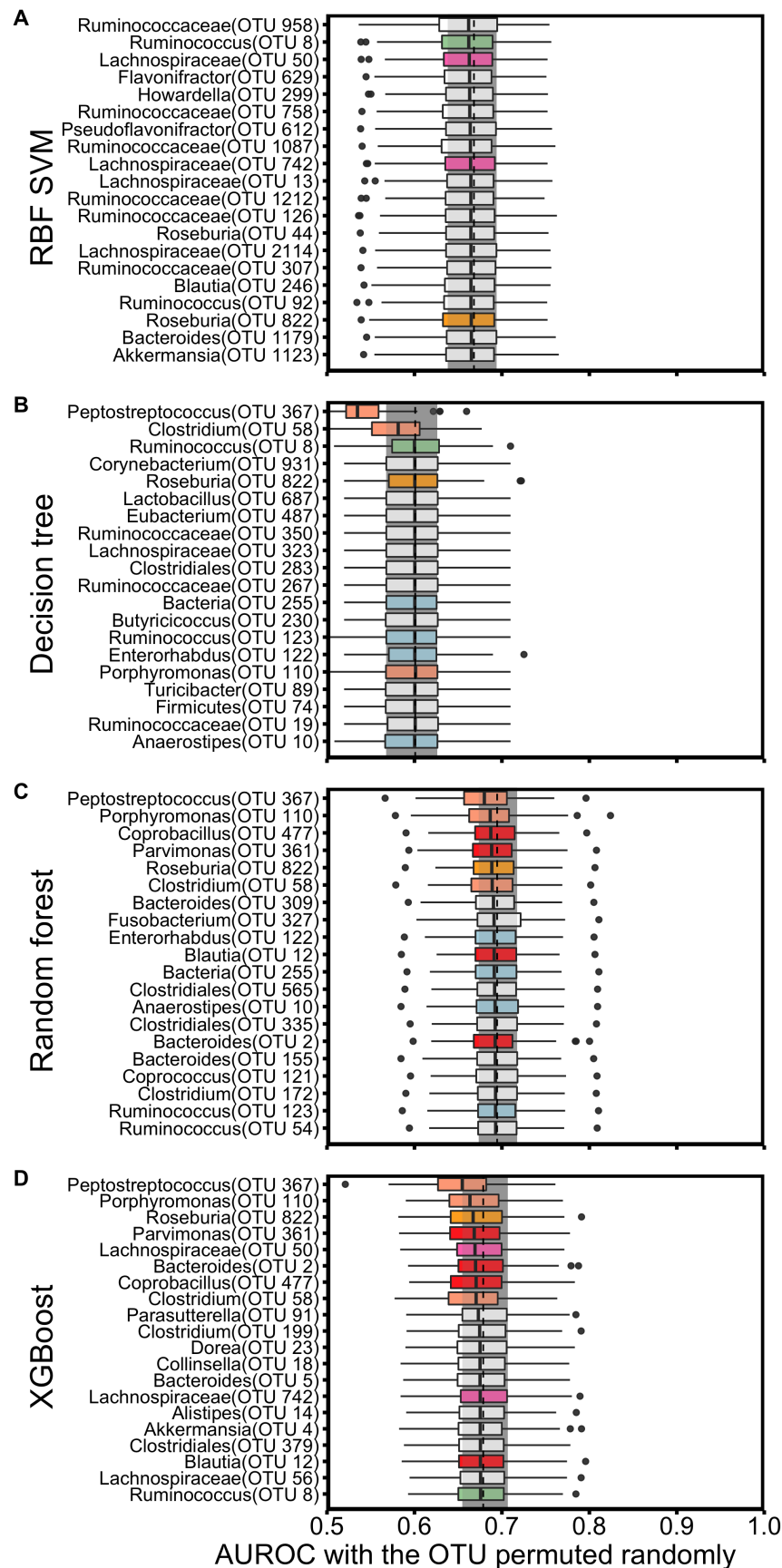


Figure 4. Interpretation of the non-linear ML models. (A) SVM with radial basis kernel, (B) decision tree, (C) random forest, and (D) XGBoost feature importances were explained using permutation importance on the held-out test data set. The gray rectangle and the dashed line show the IQR range and median of the base testing AUROC without any permutation. The colors of the box plots represent the OTUs that were shared among the different models; yellow were OTUs that were shared among all the non-linear models, salmon were OTUs that were shared among the tree-based models, green were the OTUs shared among SVM with radial basis kernel, decision tree and XGBoost, pink were the OTUs shared among SVM with radial basis kernel and XGBoost only, red were the OTUs shared among random forest and XGBoost only and blue were the OTUs shared among decision tree and random forest only. For all of the tree-based models, a *Peptostreptococcus* species (OTU00367) had the largest impact on predictive performance.

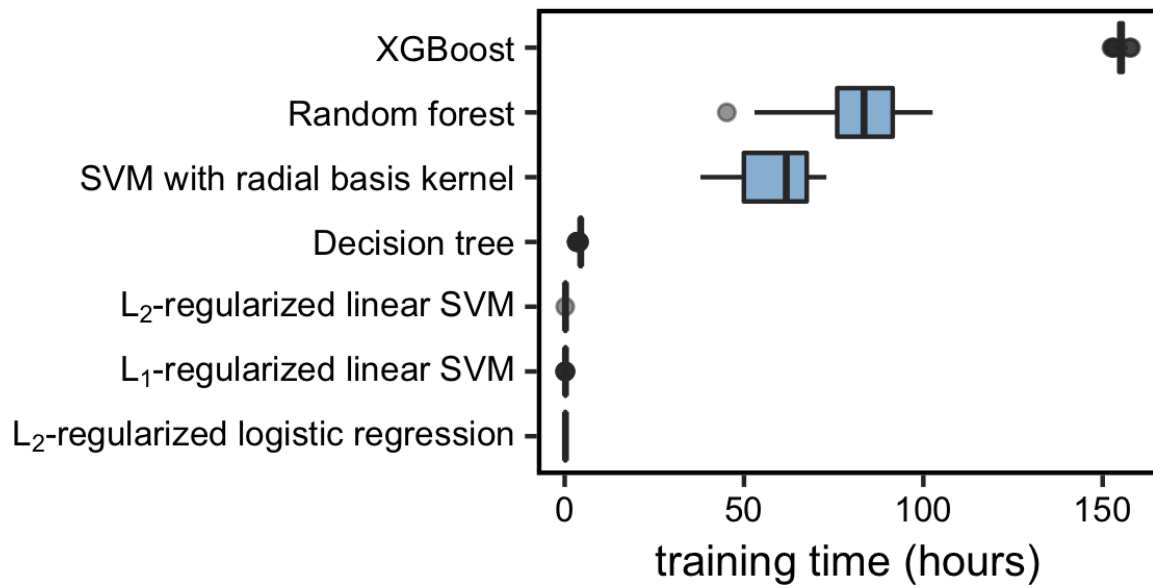
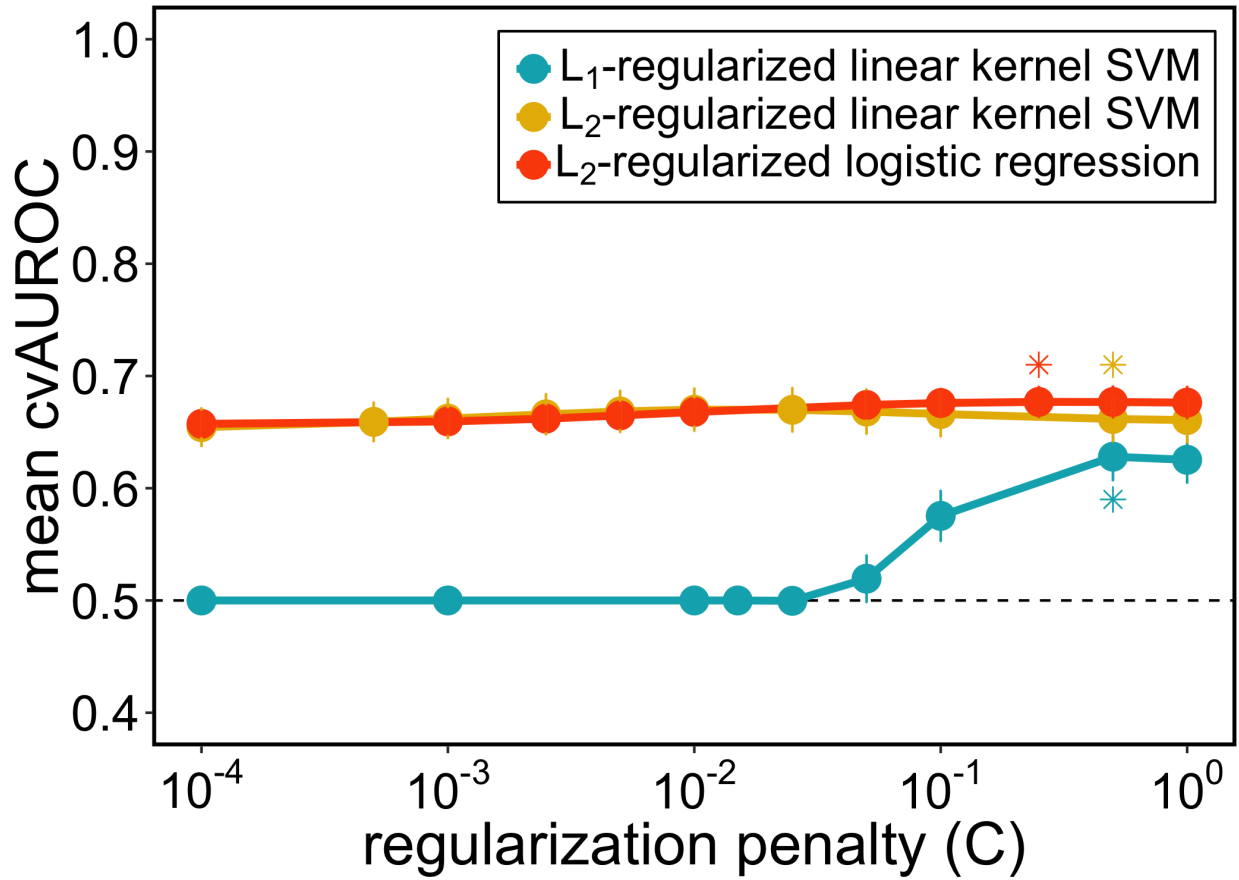


Figure 5. Training times of seven ML models. The median training time was the highest for XGBoost and shortest for L2-regularized logistic regression.



384

385 **Figure S1. Hyperparameter setting performances for linear models.** (A) L2 logistic regression,
 386 (B) L1 SVM with linear kernel, and (C) L2 SVM with linear kernel mean cross-validation AUROC
 387 values when different hyperparameters were used in training the model. The stars represent the
 388 highest performing hyperparameter setting for each model.

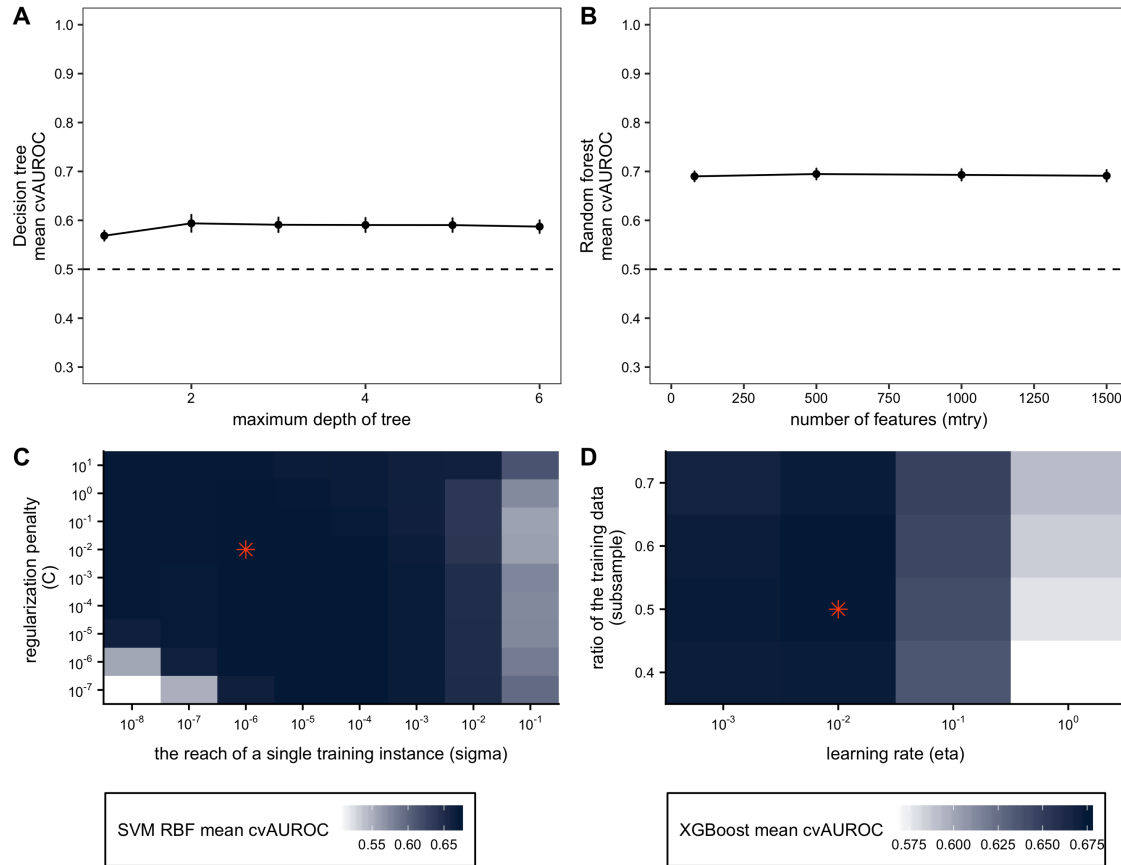


Figure S2. Hyperparameter setting performances for non-linear models. (A) Decision tree, (B) Random forest, (C) SVM with radial basis kernel, and (D) XGBoost mean cross-validation AUROC values when different hyperparameters were used in training the model. The stars represent the highest performing hyperparameter setting for the models.

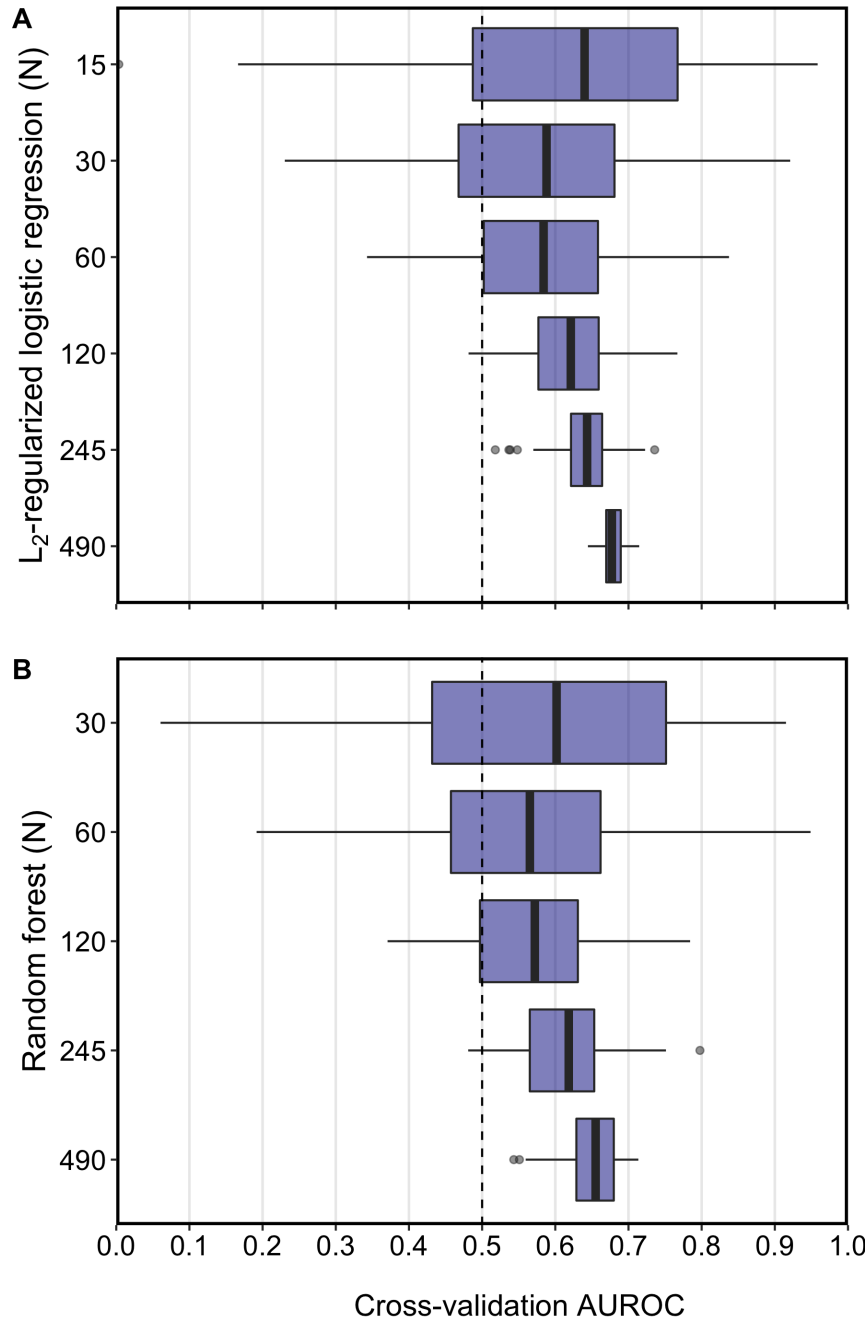


Figure S3. Classification performance of ML models across cross validation when trained on a subset of th dataset. (A) L2-regularized logistic regression and (B) Random forest models were trained using the original study design with 490 subjects and subsets of it with 15, 30, 60, 120, and 245 subjects. The range among the cross-validation AUROC values within both models at lower sample sizes were much larger than when the full collection of samples was used to train and validate the models, but included the ranges observed with the more complete datasets.

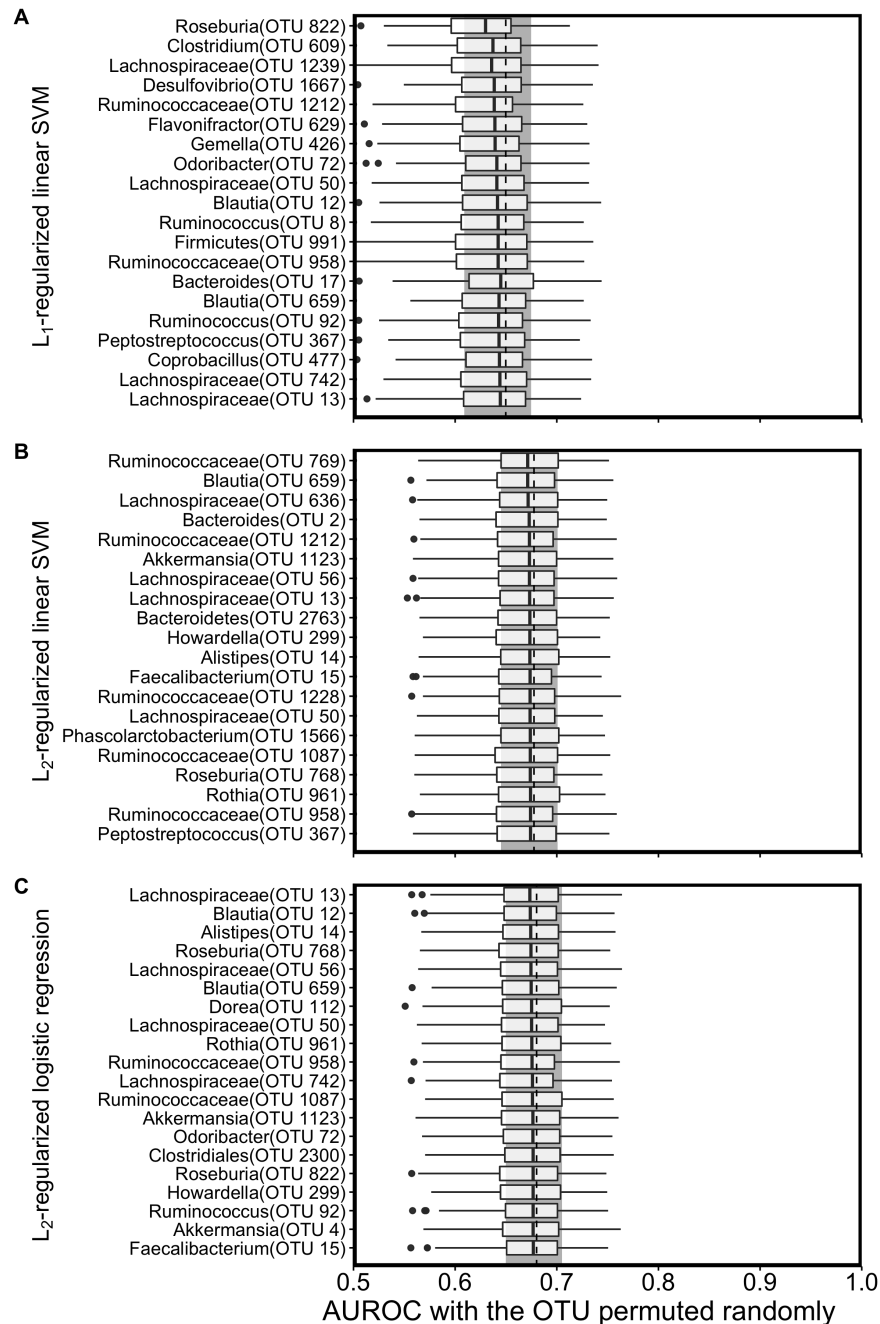


Figure S4. Interpretation of the linear ML models with permutation importance. (A) L1-regularized SVM with linear kernel, (B) L2-regularized SVM with linear kernel, and (C) L2-regularized logistic regression were interpreted using permutation importance using held-out test set.

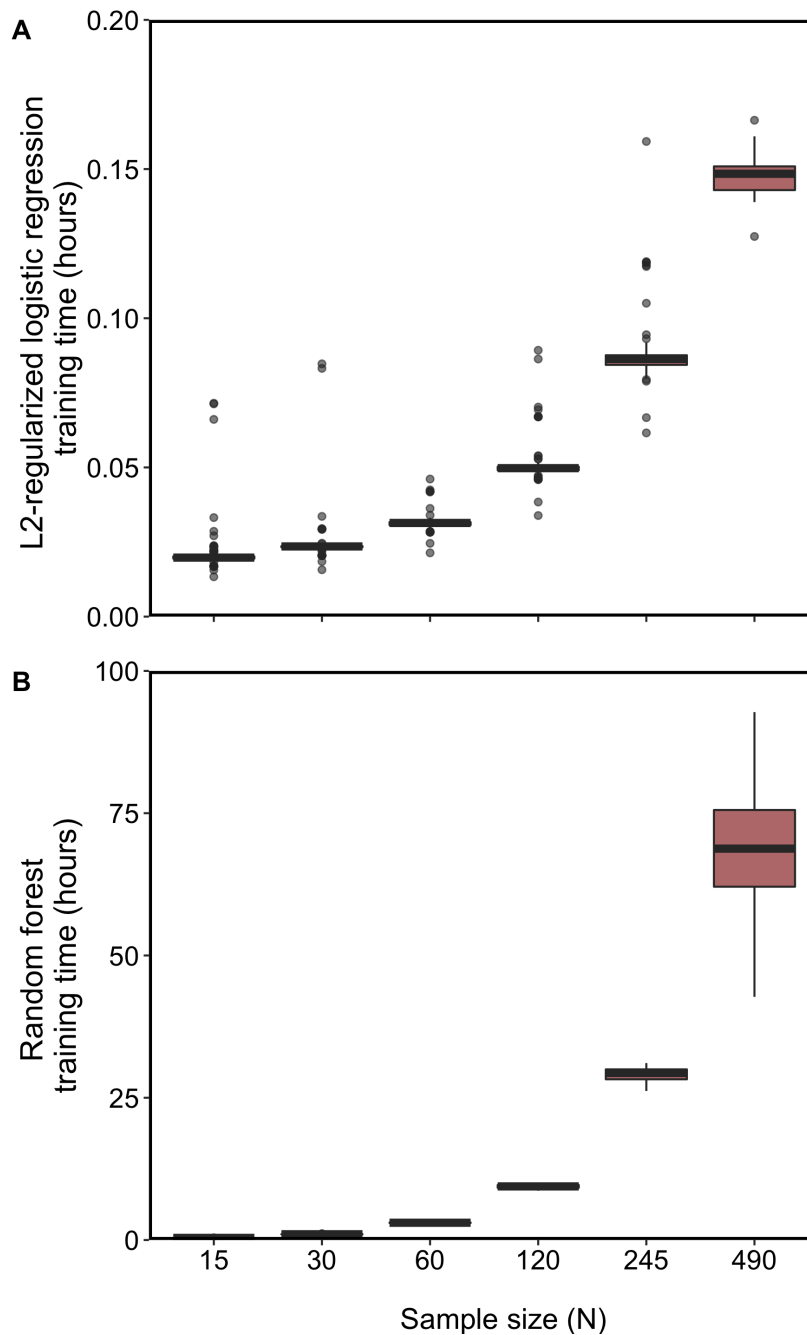


Figure S5. Training times of ML models when dataset is subsetting . (A) L2-regularized logistic regression and (B) Random forest models were trained using the original study design with 490 subjects and subsets of it with 15, 30, 60, 120, and 245 subjects. As the size of the dataset increased, the training times for L2-regularized logistic regression and random forest models increased linearly.

Table 1. Characteristics of the machine learning models in our comparative study.

Model	Description	Linearity
Logistic regression	A predictive regression analysis when the dependent variable is binary.	Linear
SVM with linear kernel	A classifier that is defined by an optimal linear separating hyperplane that discriminates between labels.	Linear
SVM with radial basis kernel	A classifier that is defined by an optimal Gaussian separating hyperplane that discriminates between labels.	Non-linear
Decision tree	A classifier that sorts samples down from the root to the leaf node where an attribute is tested to discriminate between labels.	Non-linear
Random forest	A classifier that is an ensemble of decision trees that grows randomly with subsampled data.	Non-linear
XGBoost	A classifier that is an ensemble of decision trees that grows greedily.	Non-linear

* Explainable models are not inherently interpretable but can be explained with post-hoc analyses.

Table S1. An aspirational rubric for evaluating the rigor of ML practices.

Practice	Good	Better	Best
Problem definition	Have we clearly stated the ML task? Do we have a priori hypotheses? Do we know the predictions a domain expert would make manually?	Do we know the motivation for solving the problem? How much interpretability does the problem need?	Do we know the correlated features?
Classification algorithm	Do we know the candidate algorithms for the ML problem?	Do we know our computational resources to fully train each model?	How much interpretability does the problem need? How much each candidate algorithm can provide?
ML pipeline preparation	Did we do cross-validation?	Do we have a held-out test dataset?	Have we tested our model on many different datasets?
Hyperparameter selection	Do we know the different hyperparameters each model can use and why?	Did we use historically effective hyperparameters?	Did we search the full grid space and optimized our model?
Model evaluation	Have we chosen an appropriate metric to evaluate predictive performance?	Have we reported the predictive performance on a held-out test data?	Have we provided an average predictive performance of many model runs?
Model interpretation	Do we know if our model is interpretable?	If the model is not interpretable, do we know how to explain it? Have we checked for the effect of correlated features?	Have we generated new hypotheses based on model interpretation to test model results?

References

1. **Zeller G, Tap J, Voigt AY, Sunagawa S, Kultima JR, Costea PI, Amiot A, Böhm J, Brunetti F, Habermann N, Hercog R, Koch M, Luciani A, Mende DR, Schneider MA, Schrotz-King P, Tournigand C, Tran Van Nhieu J, Yamada T, Zimmermann J, Benes V, Kloor M, Ulrich CM, Knebel Doeberitz M von, Sobhani I, Bork P.** 2014. Potential of fecal microbiota for early-stage detection of colorectal cancer. *Mol Syst Biol* **10**. doi:10.15252/msb.20145645.
2. **Zackular JP, Rogers MAM, Ruffin MT, Schloss PD.** 2014. The human gut microbiome as a screening tool for colorectal cancer. *Cancer Prev Res* **7**:1112–1121. doi:10.1158/1940-6207.CAPR-14-0129.
3. **Baxter NT, Koumpouras CC, Rogers MAM, Ruffin MT, Schloss PD.** 2016. DNA from fecal immunochemical test can replace stool for detection of colonic lesions using a microbiota-based model. *Microbiome* **4**. doi:10.1186/s40168-016-0205-y.
4. **Baxter NT, Ruffin MT, Rogers MAM, Schloss PD.** 2016. Microbiota-based model improves the sensitivity of fecal immunochemical test for detecting colonic lesions. *Genome Medicine* **8**:37. doi:10.1186/s13073-016-0290-3.
5. **Hale VL, Chen J, Johnson S, Harrington SC, Yab TC, Smyrk TC, Nelson H, Boardman LA, Druliner BR, Levin TR, Rex DK, Ahnen DJ, Lance P, Ahlquist DA, Chia N.** 2017. Shifts in the fecal microbiota associated with adenomatous polyps. *Cancer Epidemiol Biomarkers Prev* **26**:85–94. doi:10.1158/1055-9965.EPI-16-0337.
6. **Pasolli E, Truong DT, Malik F, Waldron L, Segata N.** 2016. Machine learning meta-analysis of large metagenomic datasets: Tools and biological insights. *PLoS Comput Biol* **12**. doi:10.1371/journal.pcbi.1004977.
7. **Sze MA, Schloss PD.** 2016. Looking for a signal in the noise: Revisiting obesity and the microbiome. *mBio* **7**. doi:10.1128/mBio.01018-16.
8. **Walters WA, Xu Z, Knight R.** 2014. Meta-analyses of human gut microbes associated with obesity and IBD. *FEBS Lett* **588**:4223–4233. doi:10.1016/j.febslet.2014.09.039.
9. **Vázquez-Baeza Y, Gonzalez A, Xu ZZ, Washburne A, Herfarth HH, Sartor RB, Knight R.** 2018. Guiding longitudinal sampling in IBD cohorts. *Gut* **67**:1743–1745. doi:10.1136/gutjnl-2017-315352.
10. **Qin N, Yang F, Li A, Prifti E, Chen Y, Shao L, Guo J, Le Chatelier E, Yao J, Wu L, Zhou J, Ni S, Liu L, Pons N, Batto JM, Kennedy SP, Leonard P, Yuan C, Ding W, Chen Y, Hu X, Zheng B, Qian G, Xu W, Ehrlich SD, Zheng S, Li L.** 2014. Alterations of the human gut microbiome in liver cirrhosis. *Nature* **513**:59–64. doi:10.1038/nature13568.
11. **Geman O, Chiuchisan I, Covasa M, Doloc C, Milici M-R, Milici L-D.** 2018. Deep learning tools for human microbiome big data, pp. 265–275. *In* Balas, VE, Jain, LC, Balas, MM (eds.), *Soft computing*

applications. Springer International Publishing.

12. **Thaiss CA, Itav S, Rothschild D, Meijer MT, Levy M, Moresi C, Dohnalová L, Braverman S, Rozin S, Malitsky S, Dori-Bachash M, Kuperman Y, Biton I, Gertler A, Harmelin A, Shapiro H, Halpern Z, Aharoni A, Segal E, Elinav E.** 2016. Persistent microbiome alterations modulate the rate of post-dieting weight regain. *Nature* **540**:544–551. doi:10.1038/nature20796.

13. **Dadkhah E, Sikaroodi M, Korman L, Hardi R, Baybick J, Hanzel D, Kuehn G, Kuehn T, Gillevet PM.** 2019. Gut microbiome identifies risk for colorectal polyps. *BMJ Open Gastroenterology* **6**:e000297. doi:10.1136/bmjgast-2019-000297.

14. **Flemer B, Warren RD, Barrett MP, Cisek K, Das A, Jeffery IB, Hurley E, O’Riordain M, Shanahan F, O’Toole PW.** 2018. The oral microbiota in colorectal cancer is distinctive and predictive. *Gut* **67**:1454–1463. doi:10.1136/gutjnl-2017-314814.

15. **Montassier E, Al-Ghalith GA, Ward T, Corvec S, Gastinne T, Potel G, Moreau P, Cochetiere MF de la, Batard E, Knights D.** 2016. Pretreatment gut microbiome predicts chemotherapy-related bloodstream infection. *Genome Medicine* **8**:49. doi:10.1186/s13073-016-0301-4.

16. **Ai L, Tian H, Chen Z, Chen H, Xu J, Fang J-Y.** 2017. Systematic evaluation of supervised classifiers for fecal microbiota-based prediction of colorectal cancer. *Oncotarget* **8**:9546–9556. doi:10.18632/oncotarget.14488.

17. **Dai Z, Coker OO, Nakatsu G, Wu WKK, Zhao L, Chen Z, Chan FKL, Kristiansen K, Sung JJY, Wong SH, Yu J.** 2018. Multi-cohort analysis of colorectal cancer metagenome identified altered bacteria across populations and universal bacterial markers. *Microbiome* **6**:70. doi:10.1186/s40168-018-0451-2.

18. **Mossotto E, Ashton JJ, Coelho T, Beattie RM, MacArthur BD, Ennis S.** 2017. Classification of paediatric inflammatory bowel disease using machine learning. *Scientific Reports* **7**. doi:10.1038/s41598-017-02606-2.

19. **Wong SH, Kwong TNY, Chow T-C, Luk AKC, Dai RZW, Nakatsu G, Lam TYT, Zhang L, Wu JCY, Chan FKL, Ng SSM, Wong MCS, Ng SC, Wu WKK, Yu J, Sung JJY.** 2017. Quantitation of faecal fusobacterium improves faecal immunochemical test in detecting advanced colorectal neoplasia. *Gut* **66**:1441–1448. doi:10.1136/gutjnl-2016-312766.

20. **Statnikov A, Henaff M, Narendra V, Konganti K, Li Z, Yang L, Pei Z, Blaser MJ, Aliferis CF, Alekseyenko AV.** 2013. A comprehensive evaluation of multcategory classification methods for microbiomic data. *Microbiome* **1**:11. doi:10.1186/2049-2618-1-11.

21. **Knights D, Costello EK, Knight R.** 2011. Supervised classification of human microbiota. *FEMS Microbiology Reviews* **35**:343–359. doi:10.1111/j.1574-6976.2010.00251.x.

22. **Wirbel J, Pyl PT, Kartal E, Zych K, Kashani A, Milanese A, Fleck JS, Voigt AY, Palleja A,**

- Ponnudurai R, Sunagawa S, Coelho LP, Schrotz-King P, Vogtmann E, Habermann N, Niméus E, Thomas AM, Manghi P, Gandini S, Serrano D, Mizutani S, Shiroma H, Shiba S, Shibata T, Yachida S, Yamada T, Waldron L, Naccarati A, Segata N, Sinha R, Ulrich CM, Brenner H, Arumugam M, Bork P, Zeller G.** 2019. Meta-analysis of fecal metagenomes reveals global microbial signatures that are specific for colorectal cancer. *Nature Medicine* **25**:679. doi:10.1038/s41591-019-0406-6.
- 23. Vangay P, Hillmann BM, Knights D.** 2019. Microbiome learning repo (ML repo): A public repository of microbiome regression and classification tasks. *Gigascience* **8**. doi:10.1093/gigascience/giz042.
- 24. Galkin F, Aliper A, Putin E, Kuznetsov I, Gladyshev VN, Zhavoronkov A.** 2018. Human microbiome aging clocks based on deep learning and tandem of permutation feature importance and accumulated local effects. *bioRxiv*. doi:10.1101/507780.
- 25. Reiman D, Metwally A, Dai Y.** 2017. Using convolutional neural networks to explore the microbiome, pp. 4269–4272. *In* 2017 39th annual international conference of the IEEE engineering in medicine and biology society (EMBC).
- 26. Fioravanti D, Giarratano Y, Maggio V, Agostinelli C, Chierici M, Jurman G, Furlanello C.** 2017. Phylogenetic convolutional neural networks in metagenomics. *arXiv:170902268 [cs, q-bio]*.
- 27. Thomas AM, Manghi P, Asnicar F, Pasolli E, Armanini F, Zolfo M, Beghini F, Manara S, Karcher N, Pozzi C, Gandini S, Serrano D, Tarallo S, Francavilla A, Gallo G, Trompetto M, Ferrero G, Mizutani S, Shiroma H, Shiba S, Shibata T, Yachida S, Yamada T, Wirbel J, Schrotz-King P, Ulrich CM, Brenner H, Arumugam M, Bork P, Zeller G, Cordero F, Dias-Neto E, Setubal JC, Tett A, Pardini B, Rescigno M, Waldron L, Naccarati A, Segata N.** 2019. Metagenomic analysis of colorectal cancer datasets identifies cross-cohort microbial diagnostic signatures and a link with choline degradation. *Nature Medicine* **25**:667. doi:10.1038/s41591-019-0405-7.
- 28. Rudin C.** 2018. Please stop explaining black box models for high stakes decisions. *arXiv:181110154 [cs, stat]*.
- 29. Rudin C, Ustun B.** 2018. Optimized scoring systems: Toward trust in machine learning for healthcare and criminal justice. *Interfaces* **48**:449–466. doi:10.1287/inte.2018.0957.
- 30. Knights D, Parfrey LW, Zaneveld J, Lozupone C, Knight R.** 2011. Human-associated microbial signatures: Examining their predictive value. *Cell Host Microbe* **10**:292–296. doi:10.1016/j.chom.2011.09.003.
- 31. Miller T.** 2017. Explanation in artificial intelligence: Insights from the social sciences. *arXiv:170607269 [cs]*.
- 32. Ribeiro MT, Singh S, Guestrin C.** 2016. “Why should i trust you?”: Explaining the predictions of any

classifier. arXiv:160204938 [cs, stat].

33. **Nori H, Jenkins S, Koch P, Caruana R.** 2019. InterpretML: A unified framework for machine learning interpretability. arXiv:190909223 [cs, stat].

34. **Sze MA, Schloss PD.** 2018. Leveraging existing 16S rRNA gene surveys to identify reproducible biomarkers in individuals with colorectal tumors. *mBio* **9**:e00630–18. doi:10.1128/mBio.00630-18.

35. **Dormann CF, Elith J, Bacher S, Buchmann C, Carl G, Carré G, Marquéz JRG, Gruber B, Lafourcade B, Leitão PJ, Münkemüller T, McClean C, Osborne PE, Reineking B, Schröder B, Skidmore AK, Zurell D, Lautenbach S.** 2013. Collinearity: A review of methods to deal with it and a simulation study evaluating their performance. *Ecography* **36**:27–46. doi:10.1111/j.1600-0587.2012.07348.x.

36. **Sze MA, Topçuoğlu BD, Lesniak NA, Ruffin MT, Schloss PD.** 2019. Fecal short-chain fatty acids are not predictive of colonic tumor status and cannot be predicted based on bacterial community structure. *mBio* **10**:e01454–19. doi:10.1128/mBio.01454-19.

37. **Kocheturov A, Pardalos PM, Karakitsiou A.** 2019. Massive datasets and machine learning for computational biomedicine: Trends and challenges. *Ann Oper Res* **276**:5–34. doi:10.1007/s10479-018-2891-2.

38. **Kim M, Oh I, Ahn J.** 2018. An improved method for prediction of cancer prognosis by network learning. *Genes* **9**:478. doi:10.3390/genes9100478.

39. **Schloss PD, Westcott SL, Ryabin T, Hall JR, Hartmann M, Hollister EB, Lesniewski RA, Oakley BB, Parks DH, Robinson CJ, Sahl JW, Stres B, Thallinger GG, Van Horn DJ, Weber CF.** 2009. Introducing mothur: Open-Source, Platform-Independent, Community-Supported Software for Describing and Comparing Microbial Communities. *Appl Environ Microbiol* **75**:7537–7541.

40. **Westcott SL, Schloss PD.** 2017. OptiClust, an Improved Method for Assigning Amplicon-Based Sequence Data to Operational Taxonomic Units. *mSphere* **2**. doi:10.1128/mSphereDirect.00073-17.

41. **Rognes T, Flouri T, Nichols B, Quince C, Mahé F.** 2016. VSEARCH: A versatile open source tool for metagenomics. *PeerJ* **4**:e2584. doi:10.7717/peerj.2584.

42. **Li L, Jamieson K, DeSalvo G, Rostamizadeh A, Talwalkar A.** 2016. Hyperband: A novel bandit-based approach to hyperparameter optimization. arXiv:160306560 [cs, stat].